Comparison of the magnetic properties of GaInAs/MnAs and GaAs/MnAs hybrids with random and ordered arrangements of MnAs nanoclusters

M. T. Elm,[1,a)] C. Michel,[1] J. Stehr,[1] D. M. Hofmann,[1] P. J. Klar,[1] S. Ito,[2] S. Hara,[2] and H.-A. Krug von Nidda[3]
[1]*Institute of Experimental Physics I, Justus-Liebig University, Heinrich-Buff-Ring 16, 35392 Giessen, Germany*
[2]*Research Center for Integrated Quantum Electronics, Hokkaido University, Sapporo 060-8628, Japan*
[3]*Experimentalphysik V, University of Augsburg, 86159 Augsburg, Germany*

(Received 6 October 2009; accepted 19 November 2009; published online 4 January 2010)

Random arrangements of ferromagnetic MnAs nanoclusters were deposited on (111)B-GaInAs surfaces by standard metal-organic vapor-phase epitaxy (MOVPE). Ordered arrangements of MnAs nanoclusters and cluster chains were obtained by selective-area MOVPE on prepatterned (111)B-GaAs substrates. This new method enables one to control the arrangement of nanoclusters in the growth process offering interesting opportunities to tune the properties of individual MnAs clusters as well as the interaction between the carriers in the surrounding semiconductor matrix and the clusters. The magnetic anisotropy of the MnAs clusters was investigated by magnetic force microscopy and ferromagnetic resonance measurements. The in-plane magnetic anisotropy is mainly determined by the interplay of cluster shape and magnetocrystalline anisotropy while the hard magnetic axis of the clusters is perpendicular to the sample plane independent of cluster shape. The magnetotransport measurements demonstrate that the cluster arrangements strongly influence the transport properties. © *2010 American Institute of Physics*. [doi:10.1063/1.3275427]

I. INTRODUCTION

Magnetoelectronic devices are of great interest as they offer extended functionality, e.g., the nonvolatility of stored information in magnetic random access memories. All devices used today, which are based on the tunneling magnetoresistance (TMR)[1] or the giant magnetoresistance (GMR)[2,3] effect, are mostly operated in a vertical device geometry where the current flow is applied perpendicular to the layer planes. This, however, hinders integration of these devices into larger planar structures, leads to complicated device architectures, and limits device miniaturization.

An interesting alternative are granular hybrid structures where ferromagnetic nanoclusters are embedded in a semiconducting matrix, which show magnetoresistance (MR) effects similar to the GMR and TMR effect.[4,5] Additionally their properties can be tuned in a wide range. This tunability arises from the large number of degrees of freedom, e.g., the mean distance between the clusters, the cluster size, and the cluster shape. However, a major obstacle in employing such hybrid structures is the random distribution of the clusters in the host material which leads to significant variations in the transport properties. Therefore the technological application of granular materials has been mainly restricted to macroscopic devices, which allow one to take advantage of the tunability of the hybrid's properties while avoiding problems due to statistical fluctuations in cluster size, number, etc. This suggest that a miniaturization of devices built of conventionally synthesized granular hybrids where the clusters are arranged randomly in the matrix will probably play no role in the long run for nanoelectronics.

In contrast, the new method of selective-area growth of self-assembled MnAs nanoclusters on prepatterned (111)B-GaAs substrates has the potential to overcome the disorder problem by controlling size, shape, and position of the nanoclusters. Controlling the spatial arrangement of clusters on the sample surface allows one to actively tune the structure of individual clusters in order to optimize the properties of the samples for magnetoelectronic devices.

In this paper, we present results of the growth of randomly arranged hexagon-shaped ferromagnetic MnAs nanoclusters by standard metal-organic vapor-phase epitaxy (MOVPE) as well as of the growth of ordered arrangements of elongated nanoclusters (length 690 nm, width 290 nm) and cluster chains by selective-area MOVPE (SAMOVPE). The magnetic properties of the nanoclusters were investigated by magnetic force microscopy (MFM) and ferromagnetic resonance measurements (FMR). The influence of the cluster arrangements on the magnetotransport properties of the surrounding matrix were investigated and correlated with the properties of the cluster ensembles.

II. EXPERIMENTAL DETAILS

Zincblende III-V (111) substrates are well suited for the growth of the NiAs-type MnAs nanoclusters. The reason is that the (111) plane matches well the c-plane of hexagonal MnAs as both are of the same symmetry. For this substrate orientation, the c-axis of the NiAs-type MnAs clusters is oriented along the growth direction.

Three samples with random arrangements of hexagonal nanoclusters were grown on undoped GaInAs layers on (111)B InP substrates at a temperature of 650 °C by standard MOVPE.[6] For the series of samples, the V/Mn ratio in the

a)Electronic mail: matthias.elm@exp1.physik.uni-giessen.de.

growth process was varied leading to a variation in the cluster density. For the V/Mn ratios of 375, 750, and 1125 cluster densities of 2.8×10^8, 6.2×10^8, and 6.6×10^8 nanoclusters per cm^{-2}, respectively, were obtained. The clusters have a typical diameter of 200 nm. The Mn provided during the growth of the MnAs nanoclusters also diffuses into the undoped GaInAs surface, where it is incorporated as an acceptor yielding a p-type paramagnetic dilute magnetic semiconductor. All samples show p-type conductivity of the matrix with nearly the same carrier concentration of around 1.7×10^{18} cm^{-3} at 280 K.

In order to grow ordered arrangements of nanoclusters the (111)B GaAs substrates were partially masked with a SiO_2 thin film, which was deposited by plasma sputtering. This thin film was structured by electron-beam lithography and wet-chemical etching with buffered hydrofluoric acid such that the SiO_2 was removed at places where the MnAs nanoclusters were to be situated.[7] The resulting mask openings for elongated nanoclusters had a length of 650 nm and a width of 150 nm. In order to grow different cluster arrangements and chains the distance between individual openings in the SiO_2 layer was varied between 1.5 μm for regular arrangements of the clusters and 50 nm for the cluster chains where the clusters merge during the growth. After a thermal treatment of the GaAs wafers in the AsH_3/H_2 atmosphere at 630 °C, an AlGaAs buffer layer was grown at 800 °C for 3 min. The MnAs nanoclusters were then grown for 10 min at 825 °C.[8] As for the samples with the randomly arranged nanoclusters the growth of the MnAs clusters leads to a p-doping of the insulating (111)GaAs-substrate with Mn, also leading to paramagnetic behavior.

Superconducting quantum interference device measurements (not shown) were performed on some of the samples in order to determine the Curie-temperature T_C of the ferromagnetic nanoclusters. For all investigated samples T_C is about 340 K which is also observed for MnAs nanoclusters of conventially synthesized GaMnAs/MnAs hybrids prepared by MOVPE at high growth temperatures.[9] This is a slight enhancement of T_C with respect to bulk MnAs (T_C =318 K) which may originate from different sources, e.g., strain or the single-domain character of the clusters, or the incorporation of a small fraction of Ga atoms into the clusters.

The quality of the cluster growth was investigated by atomic force microscopy (AFM) and scanning electron microscopy (SEM). MFM was used to determine the magnetic domain structure of individual nanoclusters and of cluster chains. Prior to the MFM measurements an external magnetic field of 0.35 T was applied in order to align the magnetization of the clusters, the actual MFM measurement was performed without external magnetic field. We also studied the magnetic properties of the ensembles of MnAs clusters by FMR, where the external field was rotated in out-of-plane geometry, i.e., in the $(11\bar{2})$-plane as well as in in-plane geometry, i.e., in the (111)-plane at 150 or 280 K.

The magnetotransport measurements were performed in the temperature range from 15 to 280 K. The external magnetic field was applied perpendicular to the sample surface in a superconducting magnet system yielding external fields up to 10 T. DC currents were used varying between 5 nA and 1 μA depending on the measurement temperature and the sample under study.

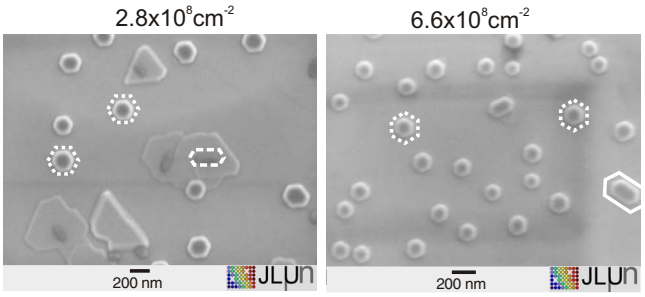

FIG. 1. (Color online) SEM images of the sample surface of the samples with the lowest (left) and highest cluster density (right). Three different cluster types were found, hexagon-shaped (dotted line), ellipsoidal clusters (dashed line), and cluster complexes (solid line).

III. RESULTS AND DISCUSSION

A. Randomly distributed hexagon-shaped MnAs nanoclusters on (111)B-InP substrates

The cluster shape of the three samples grown was investigated by SEM. The SEM images of the samples with the lowest and the highest cluster density are shown in Fig. 1. All three samples have hexagon-shaped MnAs clusters (dotted line) on the surface, which are randomly distributed. Cluster complexes (solid line) can only be observed for the sample with the highest cluster density. Such complexes arise from two cluster seeds in close vicinity, where the clusters merge during the growth process into a single elongated cluster. The other two samples also show some clusters of ellipsoidal shape (dashed line).

In order to determine the magnetic properties, FMR measurements were performed at 150 K for the sample with the highest cluster density in out-of-plane and in-plane geometry. The results are shown in Figs. 2(a) and 2(b), respectively. The out-of-plane measurement shows two resonance signals which originate from two different cluster shapes, the hexagon-shaped and the elongated nanoclusters, in concor-

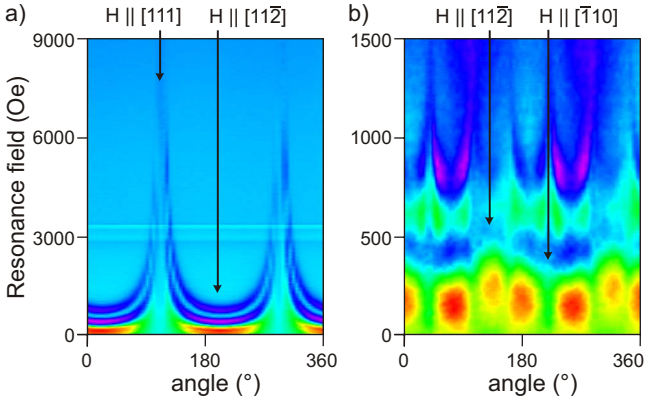

FIG. 2. (Color online) FMR at 150 K for (a) out-of-plane and (b) in-plane geometry for the sample with the highest cluster density. In out-of-plane geometry a strong 180° anisotropy can be found due to the in-plane orientation of the magnetization, while the in-plane geometry shows only a weak 60° anisotropy due to the hexagonal shape of the nanoclusters.

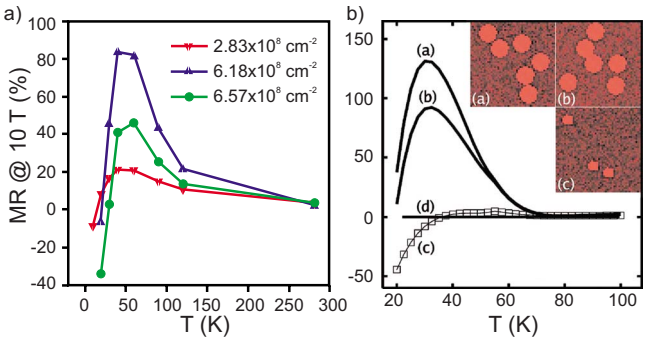

FIG. 3. (Color online) (a) Experimental results and (b) theoretical curves (Ref. 10) of the MR at 10 T of the samples with randomly distributed clusters. The cluster size and their distribution strongly influences the MR effects which is in qualitative agreement with the theoretical calculations.

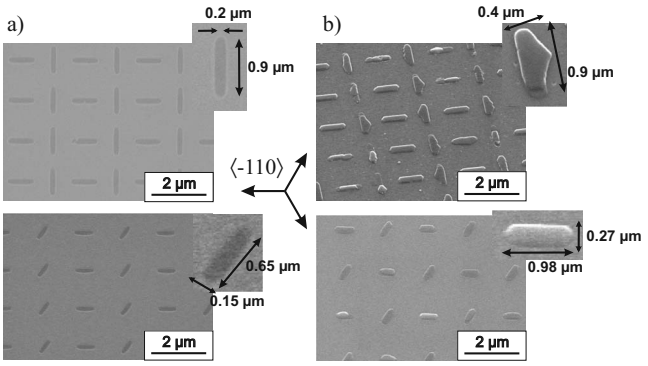

FIG. 4. SEM images of the (a) openings in the SiO_2-layer and (b) of the resulting MnAs clusters. The MnAs nanoclusters assemble in the openings keeping their crystal facets, i.e., their crystal axes grow parallel to the ⟨−110⟩-direction of the substrate.

dance with the SEM studies. In this geometry, a strong 180° anisotropy can be observed where the hard magnetic axis is orientated along the ⟨111⟩-direction, i.e., the magnetization lies in the sample plane. In in-plane geometry, the behavior of the magnetization of the MnAs clusters is weakly anisotropic exhibiting a sixfold symmetry corresponding to the hexagonal crystal symmetry and the cluster shape.

The MR behavior of all three samples was measured for an orientation of the external magnetic field perpendicular to the sample plane. The results are shown in Fig. 3(a), where the MR at 10 T is plotted versus the temperature. The MR curves of samples with random cluster distributions show positive as well as negative MR effects. At low temperatures, a negative MR is observed which increases with increasing cluster density. With increasing temperature, the negative MR effect vanishes and a positive MR becomes dominant showing the largest effect at about 50 K. A positive contribution leading to a maximum MR value of about 20% is observed for the sample with the lowest cluster density. The maximum value of the MR is 85% for the sample with the intermediate cluster density but decreases again for the highest cluster density. At higher temperatures, the positive MR of all samples vanishes. A similar behavior is commonly observed for GaMnAs/MnAs hybrid structures, where MnAs nanoclusters of different shapes are randomly distributed in the GaMnAs matrix.[5,11,12] The mechanisms of the charge transport in both hybrid systems is comparable as it occurs via holes in the p-type paramagnetic semiconductor, GaInMnAs and GaMnAs, respectively.

The negative MR effect at low temperature can be explained by trapping effects in the vicinity of the ferromagnetic MnAs clusters. The inhomogeneous stray magnetic field of a ferromagnetic MnAs cluster in conjunction with the giant Zeeman effect of the paramagnetic matrix causes a local splitting of the bands near the cluster where carriers are trapped in zero external magnetic field at low temperatures. This effect may be enhanced by the formation of a Schottky-barrier between the semiconductor matrix and the metallic MnAs cluster. By applying an external magnetic field, the trapping potential is lowered as the giant Zeeman splitting, which follows a Brillouin function, saturates at higher magnetic fields. Thus, the trapped carriers may be released leading to the negative MR effect.[5] The positive MR effect can be explained by assuming different minority and majority spins of the carriers in the matrix and in the clusters. Without an external field, the occupation numbers for both spin orientations in the matrix are equal, however, one spin orientation of the carriers (majority carriers) can pass preferably through the clusters due to their high spin polarization at the Fermi-energy. Applying a magnetic field leads to the giant Zeeman splitting in the matrix which in turn causes different occupation numbers for the two spin orientations in the paramagnetic semiconductor matrix. If the spin orientation of the majority spins in the matrix is now different from that of the clusters, then carrier transport through the clusters is suppressed, which leads to a positive MR effect. Based on these assumptions the behavior can be simulated using a network model. The details of the model can be found elsewhere.[13] Representative results of the calculations are plotted in Fig. 3(b) and are in qualitative agreement with the experimental data.[10] The calculations also predict that the MR effects strongly depend on cluster density, cluster size, and cluster arrangement. Already a minor rearrangement of the clusters can lead to strong differences in the MR behavior of miniaturized samples containing only a few nanoclusters.

B. Regularly arranged MnAs nanoclusters and chains on (111)B-GaAs substrates

We investigated the influence of the orientation of the elongated openings in the SiO_2 mask with respect to the crystal axes of the underlying (111)B-GaAs substrate. Two samples each with two types of elongated clusters were prepared. In case of the first sample, the long axes of the elongated mask openings were oriented parallel to the $\langle\bar{1}10\rangle$-axis of GaAs and perpendicular to it, along $\langle\bar{2}11\rangle$. In case of the second sample, the long axes of the elongated mask openings were oriented parallel to the $\langle\bar{1}10\rangle$-axis of GaAs and rotated by 120° about the ⟨111⟩ direction. The SEM images of the resulting openings are shown in Fig. 4(a) for both samples. Well defined openings can be seen on both samples independent of the orientation of the axis of elongation of the mask opening, as expected for the isotropic SiO_2 layers. Figure 4(b) shows the SEM images of the samples after the growth of the clusters. It can be seen that the nanoclusters assemble

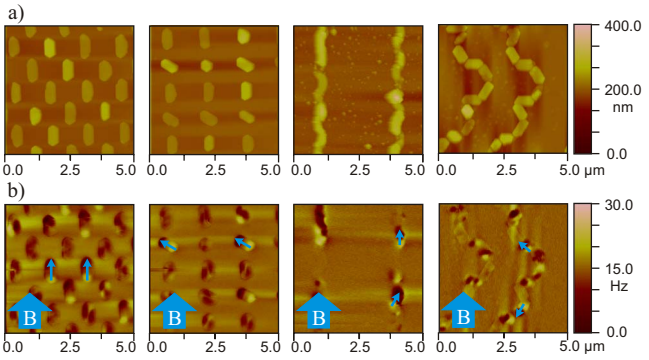

FIG. 5. (Color online) (a) AFM and (b) MFM images of different cluster arrangements (left) and cluster chains (right). The large blue arrow in the AFM images indicates the direction of the external magnetic field, while the small arrows indicate the direction of the cluster magnetization. In the MFM images it can be clearly seen that the magnetization direction at low fields is determined by the cluster shape and not by the direction of the external magnetic field.

in the openings with a well defined orientation reflected by the formation of the crystal facets, i.e., crystal axes of the clusters and of the substrate are always oriented according to a fixed crystallographic relationship.[8] In particular, it can be seen that the clusters with the axis of elongation along $\langle \bar{2}11 \rangle$ cannot reproduce the shape defined by the mask openings due to the faster growth rates on a-plane facets. Thus, it turns out that to obtain high-quality clusters with a large aspect-ratio defined by the mask openings in the SiO_2, the mask openings must be orientated parallel to the $\langle \bar{1}10 \rangle$ crystal direction of the substrate or equivalent directions arising from it by rotation by $\pm 120°$ about the $\langle 111 \rangle$ direction.

In addition, several different arrangements of elongated nanoclusters and cluster chains were grown as described above. All samples were investigated by AFM and MFM in order to determine the cluster quality and their domain structure. The results for some different arrangements are shown in Fig. 5. The AFM images show that the elongated MnAs nanoclusters [left two images in Fig. 5(a)] grow regularly in the openings and that no MnAs clusters can be found on the SiO_2 between them. On the MFM images [Fig. 5(b)] one can find, that there are some clusters exhibiting a single magnetic domain. The magnetization of the single magnetic domain clusters is always orientated along the cluster direction, i.e., an a-direction of hexagonal MnAs. At low fields the magnetization orientation is dominated by the cluster shape and not by the direction of the external magnetic field. For the growth of cluster chains (right two images in Fig. 5), the openings in the SiO_2 mask were arranged close to each other with distances of 50 nm between them. This arrangement was supposed to lead to a merging of the clusters in the growth process and to yield a chainlike arrangement of connected MnAs clusters. However, the AFM images reveal that there are still small gaps between clusters in many places. Furthermore, the MFM images show that the connected clusters and cluster chains do not grow entirely regularly.

FMR measurements were performed in order to further investigate the magnetic properties. The results for regularly arranged hexagon-shaped MnAs nanoclusters are shown in Fig. 6(a). The diameter of the clusters on the sample varies

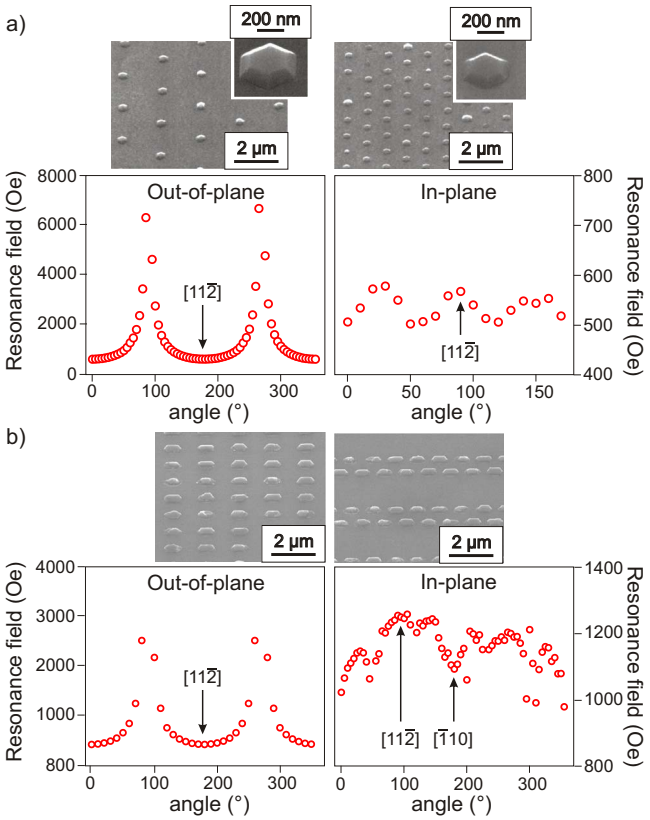

FIG. 6. (Color online) FMR at 280 K in (a) out-of-plane (left) and in-plane geometry (right) of regularly arranged hexagon-shaped nanoclusters and (b) regularly arranged elongated nanoclusters. For the out-of-plane geometry both cluster arrangements show a strong 180° anisotropy, while for the in-plane measurements a sixfold anisotropy is found. For the elongated nanoclusters this hexagonal symmetry is additionally overlaid by a weak 180° anisotropy due to asymmetric cluster shape.

between 170 nm and 1.2 μm, while the distance between the clusters varies between 1 and 3 μm. As for the randomly arranged hexagon-shaped clusters, a 180° anisotropy out-of-plane (top) and a hexagonal anisotropy in-plane (bottom) can be observed. As clusters of different diameters were measured simultaneously but only one resonance is observed in the spectra, the resonance field does not depend on cluster size but on its shape only. Figure 6(b) shows the results for the elongated nanoclusters with a length of 690 nm and a width of 250 nm. In out-of-plane geometry (top) again a twofold anisotropy is found while in in-plane geometry (bottom) the hexagonal anisotropy is overlaid by a weak 180° symmetry, which is due to the asymmetric shape of the clusters.

We also performed MR-measurements on some of the samples with regularly arranged elongated nanoclusters and cluster chains. The results are depicted in Fig. 7(a). The sample with the elongated nanoclusters shows a large MR up to 600% at low temperatures (T=15 K), which decreases rapidly with increasing temperature. At a temperature of about 20 K the MR drops to 100% and for even higher temperatures the positive MR vanishes almost entirely. The sample with the cluster chains shows a somewhat similar behavior. The positive MR reaches a value up to 600% at 15 K but in this case even at 20 K a MR effect of 450% is still observable, which again vanishes for higher temperatures.

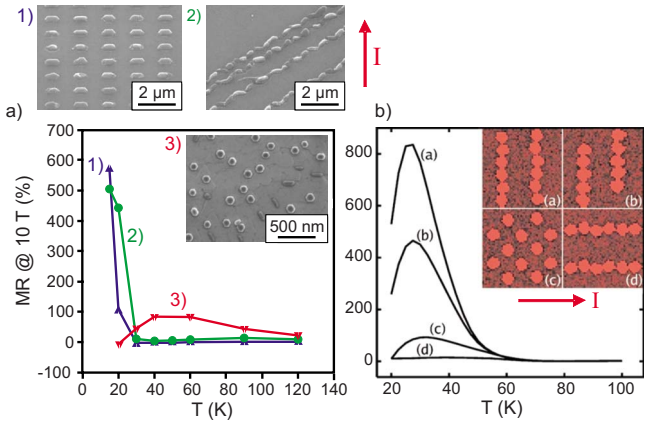

FIG. 7. (Color online) (a) Comparison of the MR of regularly arranged elongated nanoclusters, cluster chains and randomly distributed hexagon-shaped nanoclusters. Compared to the small hexagon-shaped nanoclusters the elongated clusters have a much larger effect on the transport properties. (b) Theoretical calculations of the MR with different cluster arrangements (Ref. 10) show qualitatively the same behavior.

The arrangement of elongated nanoclusters strongly influences the transport path through the matrix. The current cannot pass the nanoclusters at high magnetic field, which leads to the observed strong MR. For comparison, the MR of a sample with a random cluster distribution and a cluster density of 6.2×10^8 cm^{-2} is also shown. Here, the small clusters with a typical diameter of 200 nm have a small influence on the transport path in the matrix. The dominant current path passes through areas of the sample which are further away from the clusters. Therefore only MR effects of 100% can be observed. Figure 7(b) shows theoretical results for the MR of different cluster arrangements.[10] The calculations show that for elongated clusters [arrangements (a) and (b)] large MR effects of up to 800% can be expected. For a random cluster distribution [arrangement (c)] the MR effects are much smaller (around 100%) in qualitative agreement with experiment.

IV. SUMMARY

SAMOVPE on partially masked (111)B GaAs substrates allows one to grow ordered arrangements of MnAs nanoclusters with well defined cluster sizes, shapes, and positions on the sample. This control overcomes the problem of randomness in conventional Ga(In)MnAs/MnAs granular hybrids which was a major hindrance for the application of this class of materials in miniaturized devices. Furthermore, the control of the cluster properties allows one to tune magnetic properties as well as MR properties of the samples. The former is dominated by the interplay of shape and magnetocrystalline anisotropy of the clusters whereas the latter depends significantly on the interplay of free holes in the paramagnetic semiconductor matrix and the ferromagnetic MnAs clusters. The magnetotransport measurements are in good agreement with theoretical modeling based on a resistor network model. This shows that the MR effects in the samples can be optimized for particular needs by the arrangement of the clusters within the semiconductor matrix. The same will hold for other properties making such ordered nanocluster arrangements suitable building blocks for magnetoelectronic devices.

ACKNOWLEDGMENTS

We would like to thank the DFG and JSPS for financial support. M.T.E. would like to thank the Justus-Liebig University for funding his Ph.D. studentship.

[1] M. Julliere, Phys. Lett. A **54**, 225 (1975).
[2] P. Grünberg, R. Schreiber, Y. Pang, M. B. Brodsky, and H. Sowers, Phys. Rev. Lett. **57**, 2442 (1986).
[3] M. N. Baibich, J. M. Brotot, A. Fert, F. Nguyen Van Dau, F. Petroff, P. Eitenne, G. Creuzet, A. Friederich, and J. Chazelas, Phys. Rev. Lett. **61**, 2472 (1988).
[4] A. E. Berkowitz, J. R. Mitchell, M. J. Carey, A. P. Young, S. Zhang, F. E. Spada, F. T. Parker, A. Hutten, and G. Thomas, Phys. Rev. Lett. **68**, 3745 (1992).
[5] W. Heimbrodt, P. J. Klar, S. Ye, M. Lampalzer, C. Michel, S. D. Baranovskii, P. Thomas, and W. Stolz, J. Supercond. **18**, 315 (2005).
[6] S. Hara, D. Kawamura, H. Iguchi, J. Motohisa, and T. Fukui, J. Cryst. Growth **310**, 2390 (2008).
[7] T. Wakatsuki, S. Hara, S. Ito, D. Kawamura, and T. Fukui, Jpn. J. Appl. Phys. **48**, 04C137 (2009).
[8] S. Ito, S. Hara, T. Wakatsuki, and T. Fukui, Appl. Phys. Lett. **94**, 243117 (2009).
[9] H.-A. Nidda, T. Kurz, A. Loidl, Th. Hartmann, P. J. Klar, W. Heimbrodt, M. Lampalzer, K. Volz, and W. Stolz, J. Phys.: Condens. Matter **18**, 6071 (2006).
[10] C. Michel, M. T. Elm, B. Goldlücke, S. D. Baranovskii, P. Thomas, W. Heimbrodt, and P. J. Klar, Appl. Phys. Lett. **92**, 223119 (2008).
[11] S. Ye, P. J. Klar, Th. Hartmann, W. Heimbrodt, M. Lampalzer, S. Nau, T. Torunski, W. Stolz, T. Kurz, H.-A. Krug von Nidda, and A. Loidl, Appl. Phys. Lett. **83**, 3927 (2003).
[12] P. J. Wellmann, J. M. Garcia, J.-L. Feng, and P. M. Petroff, Appl. Phys. Lett. **73**, 3291 (1998).
[13] C. Michel, P. J. Klar, S. D. Baranovskii, and P. Thomas, Phys. Rev. B **69**, 165211 (2004).